Tailoring a Solvent-Assisted Method for Solid-Supported Hybrid Lipid−Polymer Membranes

Stefano Di Leone,[||] Myrto Kyropoulou,[||] Julian Köchlin, Riccardo Wehr, Wolfgang P. Meier,* and Cornelia G. Palivan*

ACCESS | 📊 Metrics & More | 📖 Article Recommendations | 🆂�ℹ Supporting Information

ABSTRACT: Combining amphiphilic block copolymers and phospholipids opens new opportunities for the preparation of artificial membranes. The chemical versatility and mechanical robustness of polymers together with the fluidity and biocompatibility of lipids afford hybrid membranes with unique properties that are of great interest in the field of bioengineering. Owing to its straightforwardness, the solvent-assisted method (SA) is particularly attractive for obtaining solid-supported membranes. While the SA method was first developed for lipids and very recently extended to amphiphilic block copolymers, its potential to develop hybrid membranes has not yet been explored. Here, we tailor the SA method to prepare solid-supported polymer−lipid hybrid membranes by combining a small library of amphiphilic diblock copolymers poly(dimethyl siloxane)−poly(2-methyl-2-oxazoline) and poly(butylene oxide)-*block*−poly(glycidol) with phospholipids commonly found in cell membranes including 1,2-dihexadecanoyl-*sn*-glycero-3-phosphocholine, 1-palmitoyl-2-oleoyl-*sn*-glycero-3-phosphoethanolamine, sphingomyelin, and 1,2-dioleoyl-*sn*-glycero-3-phosphoethanolamine-*N*-(glutaryl). The optimization of the conditions under which the SA method was applied allowed for the formation of hybrid polymer−lipid solid-supported membranes. The real-time formation and morphology of these hybrid membranes were evaluated using a combination of quartz crystal microbalance and atomic force microscopy. Depending on the type of polymer−lipid combination, significant differences in membrane coverage, formation of domains, and quality of membranes were obtained. The use of the SA method for a rapid and controlled formation of solid-supported hybrid membranes provides the basis for developing customized artificial hybrid membranes.
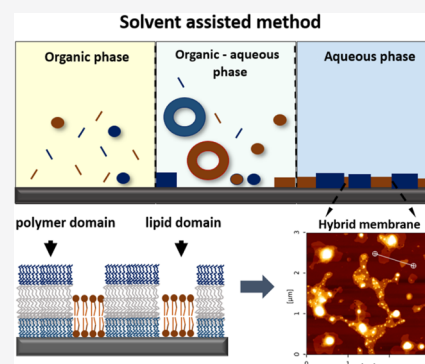
1. INTRODUCTION

The design of synthetic membranes able to mimic the structure and function of natural cell membranes is the focus of multidisciplinary research[1−5] due to their potential for a large variety of applications,[6,7] such as molecular recognition and sequencing,[8,9] biosensing,[1,10] surface coating,[11] and microelectronics.[12,13] Among the various types of synthetic membranes, the hybrid ones, consisting of amphiphilic block copolymers and phospholipids, are particularly attractive[14−16] because they combine the key advantages of each component: the chemical stability and versatility of block copolymers[17−19] with the flexibility of lipids.[20] Additionally, as hybrid membranes feature "lipid raftlike" characteristics, they are promising candidates for selective anchoring of biomolecules onto the lipid or polymer domains and the development of versatile membranes with specific biofunctionality.[21−24] Of particular interest for applications are solid-supported membranes because they have increased stability over time compared to free-standing membranes.[25−27] However, in the case of hybrid membranes, when the polymer domain of the membrane interacts with the lipid one, the resulting morphology is governed by various factors, including the charge of each component, the mean size of amphiphiles, and

the molar ratio of the involved components.[14,15,22,23] The size mismatch between the hydrophobic block of the copolymers and the lipid tails can affect the formation and structure of hybrid membranes in two possible ways: (i) elastic deformation of the hydrophobic polymer blocks due to their adaptable chain conformation and the subsequent phase separation and creation of lipid domains within the hybrid membrane, and (ii) distribution of the lipids into the polymer membrane, forming a homogeneous mixture of components where the lipid and polymer parts cannot be distinguished. For pure lipid membranes, the physical state of lipids (related to the main chain transition temperature) is crucial.[14,28,29] However, a combination of lipids with copolymers changes the composition and the characteristics of the resulting membrane.[14,22,30] The architecture and properties of a hybrid membrane can be controlled by adjusting the miscibility/
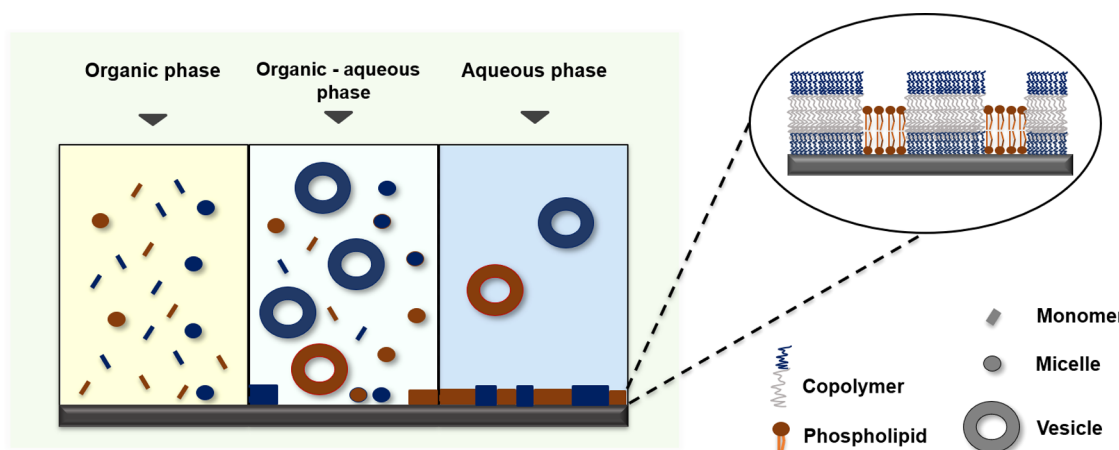
Figure 1. Schematic representation of a lipid-polymer hybrid membrane assembly formed by the solved-assisted method.

immiscibility effects that depend on the interaction between the amphiphilic copolymers and the lipids,[4,9,22,23,31] and also on the preparation method.

Solid-supported polymer and lipid membranes are produced by Langmuir–Blodgett,[32] vesicle fusion,[33,34] in the form of polymer disks,[35] tethered bilayers,[36,37] and recently reported, solvent-assisted (SA) method.[38−40] Of particular interest is the SA method as it is straightforward and requires no special equipment or complex and time-consuming sample preparation conditions.[38,40] Briefly, the amphiphilic molecules are dissolved in an organic solvent, which is then continuously replaced by an aqueous phase, which triggers the self-assembly process and induces the membrane formation. While the SA method has been previously used to generate lipid membranes[39,41] and very recently polymer membranes,[42] its potential to develop hybrid membranes has not yet been explored.

Here, we present how the SA method supports the efficient formation of solid-supported hybrid membranes by adjusting various polymer–lipid compositions (Figure 1).

We selected lipids that are normally found in cell membranes and are established components of synthetic solid-supported lipid membranes:[43] 1,2-dihexadecanoyl-*sn*-glycero-3-phosphocholine (DPPC), 1-palmitoyl-2-oleoyl-*sn*-glycero-3-phosphoethanolamine (POPE), sphingomyelin (SM), and 1,2-dioleoyl-*sn*-glycero-3-phosphoethanolamine-*N*-(glutaryl) (NGPE). As amphiphilic copolymers, we selected poly(dimethyl siloxane)−poly(2-methyl-2-oxazoline) (PDMS−PMOXA) and poly(butylene oxide)-*block*−poly-(glycidol) (PBO−PG) as both copolymers are biocompatible and have been shown to create biomimetic membranes.[5,44−46] They form highly flexible and fluid membranes because of their low glass transition temperatures and fully amorphous character. In addition, they self-assemble into planar membranes.[22,42,47] First, we monitor the real-time formation of hybrid membranes at different polymer−lipid weight ratios by quartz crystal microbalance with the dissipation module (QCM-D) and determine the average thickness, mass, and homogeneity for each hybrid membrane. We are interested in observing the formation of domains due to phase separation between the copolymers and the lipids, as reported when hybrid membranes have been obtained by the LB method.[23] We then focus on the membrane chemical composition, i.e., the intermolecular immiscibility between the lipid tails and the hydrophobic polymer blocks to understand how this induces

phase separation. While the interactions between the lipid heads and the hydrophilic blocks of copolymers play a significant role in the morphology of hybrid membranes,[48] the hydrophobic mismatch and the difference in membrane thickness represent the dominant factors resulting in lipid−polymer phase separation.[48,49] The heads of phospholipids can orient themselves toward the hydrophilic polymer blocks when hydrogen bonding or electrostatic interactions are predominant.[48] The two hydrophilic blocks used in our study are PG, which has the chemical structure and properties close to those of poly(ethylene glycol) (PEG)[50,51] and PMOXA, which is a protein-repellent, peptidomimetic polymer.[52,53] Due to the presence of hydroxyl groups in PG and the amide groups in PMOXA, these polymer blocks can only form hydrogen bonds with the lipids. Therefore, we focus here mainly on the significant hydrophobic mismatch and the difference in membrane thickness between the amphiphilic block copolymers and lipids, already reported as essential factors for the final hybrid membrane morphology in hybrid vesicles.[54−56] The morphology of the hybrid membranes and the presence of lipid rafts are characterized by atomic force microscopy (AFM). We evaluate how the SA method affects the membrane self-assembly, its physicochemical properties, and the phase domain separation between lipid and polymer domains. By systematically considering various lipid−polymer compositions and adjusting the lipid-to-polymer ratio, we optimize the hybrid membrane formation as an essential step toward highly controlled solid-supported hybrid membranes. We investigate how the hydrophobicity of the copolymer and lipid parts influence the hybrid membrane assembly. Then, we use this as an initial prediction of the membrane formation behavior when the SA method is applied to other lipid−copolymer hybrid mixtures.

2. RESULTS AND DISCUSSION

2.1. Real-Time Hybrid Membrane Formation. As the first step, we evaluated the copolymer-to-lipid weight ratio, which led to the formation of hybrid membranes with negligible defects and well-defined phase separation between the polymer and the lipid domains. The hydrophobic mismatch between phospholipids and copolymers is known to induce a rearrangement during the membrane formation to optimize the membrane structure, thus influencing its properties, such as thickness.[57] We based this optimization step on the combination of $PDMS_{61}−PMOXA_9$ copolymer
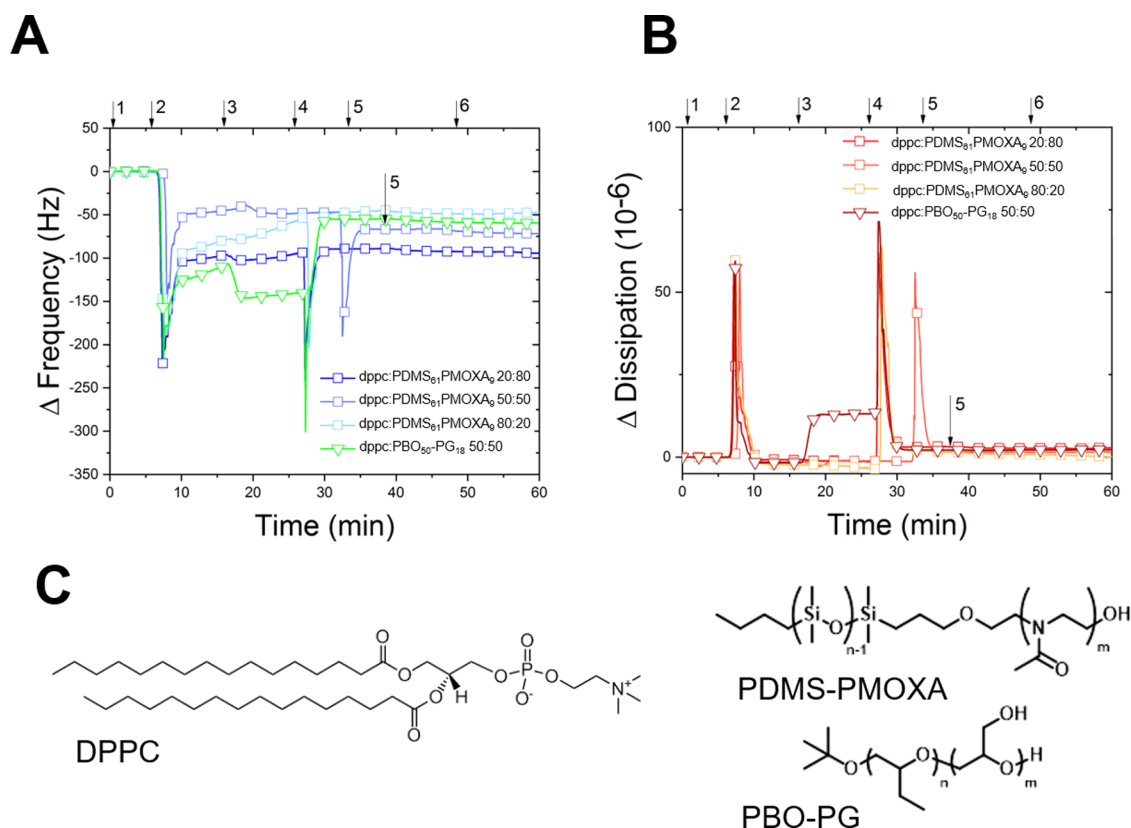
Figure 2. QCM-D plots of hybrid membrane formation: schematic representation of (A) normalized frequency shift and (B) and dissipation of DPPC lipid and PDMS−PMOXA, PBO−PG block copolymers. (C) Comparisons of different DPPC:PDMS$_{61}$−PMOXA$_9$ mixtures and DPPC:PBO$_{50}$−PG$_{18}$ in 50:50 weight ratio (↓1,4,6 = phosphate buffer saline, PBS, ↓2 = EtOH, ↓3 = polymer−DPPC solution, ↓5 = bovine serum albumin, BSA). The seventh overtone is presented.

Table 1. Frequency Shift Values for the Membrane Formation of Hybrid Membranes Composed of Different DPPC (Lipid) to PDMS-61PMOXA9 (Polymer) Ratios[a]

DPPC (% w/w)	PDMS$_{61}$-PMOXA$_9$ (% w/w)	membrane formation Δf (Hz)	surface coverage (%)	thickness (nm)
80	20	−97 ± 19	54 ± 11	9 ± 2
50	50	−83 ± 23	72 ± 22	15 ± 4
20	80	−105 ± 23	113 ± 12	18 ± 4

[a]Membrane thickness and coverage were calculated using the data recorded by QCM-D measurements.

with DPPC (Figures 2A and S1−S2). We compared three different lipid−copolymer compositions: (i) DPPC:PDMS$_{61}$−PMOXA$_9$ 80:20, (ii) DPPC:PDMS$_{61}$−PMOXA$_9$ 50:50, and (iii) DPPC:PDMS$_{61}$−PMOXA$_9$ 20:80 to find out the combination that facilitates the formation of a hybrid membrane of good quality and minor defects. We monitored the real-time hybrid membrane formation by QCM-D (Figure 2B). The calculated membrane thickness value is an average value of the polymer and lipid membrane thicknesses. By increasing the amount of copolymer, the average thickness increased from 9 ± 2 nm for the lipid−copolymer ratio of 80:20, to over 15 ± 4 nm for the lipid−copolymer ratio of 50:50, up to 18 ± 4 nm for lipid−copolymer ratio of 20:80.

We then evaluated the membrane coverage using a BSA test (Tables 1 and S1) as an established method to determine the relative area of the QCM-D silica sensor covered by a membrane.[23] In particular, BSA undergoes unspecific adsorption onto the silica substrate, which changes when a membrane is deposited on the substrate as well. The higher the amount of BSA detected on the substrate, the larger the area where the membrane failed to cover the substrate is. The membrane

coverage calculation was performed by comparing the BSA attachment onto a bare silica sensor and onto the solid substrate with deposited hybrid membranes.

As the values for the membrane coverage were satisfactory for different copolymer−lipid compositions, a good membrane quality was achieved. This membrane coverage indicates minor defects, in agreement with a previous study on copolymer solid-supported membranes.[23,32] Despite the high-frequency shift of −97 ± 19, resulting from the lipid−copolymer ratio of 80:20, the membrane coverage is the lowest at 54 ± 11, which indicates a defective membrane. In the case of the lipid−copolymer ratio of 20:80, the high amount of polymer in the mixture resulted in a quantitative coverage of 113 ± 12%. In general, a value higher than 100% stands for the full coverage of the QCM sensor. The formation of a complete monolayer with the partial formation of an additional layer increases the membrane average thickness due to the presence of membrane foldings.[41,42] The 50:50 weight ratio of DPPC and PDMS$_{61}$−PMOXA$_9$ was the one that led to the best hybrid membrane quality (minor defects, clear lipid−polymer phase separation, reproducible membrane morphology). Therefore, we kept the
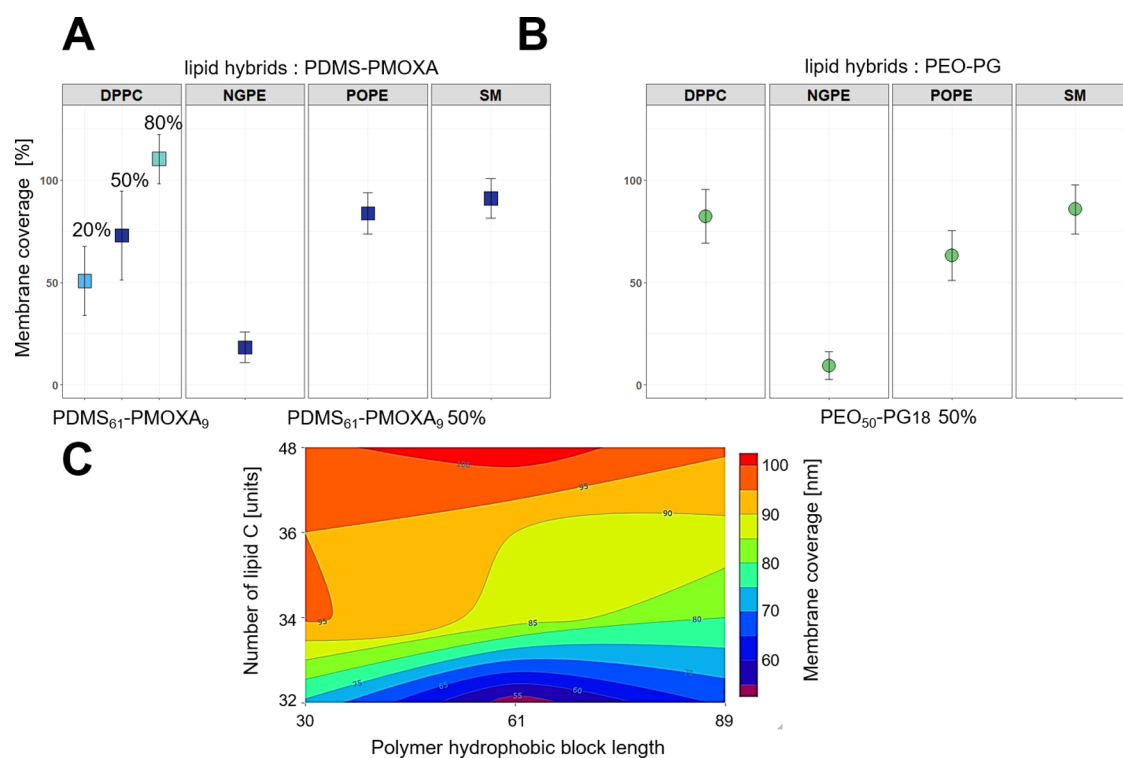
Figure 3. Scatter plot of different hybrid membranes composed of lipids and PDMS−PMOXA (A) and PBO−PG (B) copolymers. Contour plot reporting the membrane coverage as a function of the PDMS block length and the lipid number of carbon units (C).

50:50 ratio for all other lipid−copolymer combinations. We combined also DPPC and PBO_{50}-PG_{18} (Figure S3) in a 50:50 weight ratio as well (Figure 2) and obtained a hybrid membrane with an average thickness of 8 nm and a membrane coverage of 83 ± 12%. The decreased membrane thickness is due to the mean molecular area occupied by the PBO−PG and the different membrane coverage compared to the PDMS−PMOXA: DPPC membrane. We observed that a membrane coverage lower than 50% indicated a membrane with major defects, leading to inconsistent membrane thickness values. Therefore, for the experiments and analysis we conducted henceforth, we kept the lipid-to-polymer ratio at 1:1 w/w.

2.2. Hybrid Membrane Formation: Influence of the Hydrophobic Block. After optimizing the lipid-to-polymer ratio, the hybrid membrane formation was expanded to other phospholipids, components of natural membranes, together with SM, NGPE, and POPE with $PDMS_{61}$−$PMOXA_9$ and PBO_{50}−PG_{18} (Figures S4−S6). To analyze the influence of the lipid−polymer composition on the quality of the obtained solid-supported membrane, we compared the membrane coverage for the different lipids when combined with PDMS−PMOXA polymers (Figure 3A,B). It has been shown that the interaction between the polymeric and lipidic hydrophobic blocks is a determining factor for the hybrid membrane formation.[4,31,58,59] Therefore, we constructed a contour plot to associate the membrane coverage to the length of the hydrophobic block of the polymer (units) and the number of hydrophobic lipid chains (Figure 3C). As observed, a longer lipid chain decreases the chain mismatch and contributes to the formation of a planar assembly with a better membrane coverage.[4] On the other side, a long hydrophobic polymer block might favor a three-dimensional rather than a bidimensional assembly according to the curvature and packing parameter.[60−63] The best membrane

quality for the hybrid membranes obtained with this library of copolymers was found for intermediate values of the hydrophobic block length (ca. 60 units).

Additionally, the average thickness of the hybrid membrane is determined as a function of the lipid and PDMS−PMOXA polymer hydrophobicity (measured in units of hydrophobic blocks for the copolymer and carbon units in the lipid chains), respectively (Figure S7A). It has to be noted that a low membrane coverage automatically biases the calculated membrane thickness. We represented the influence of different lipids combined with the PBO−PG polymer on membrane thickness and coverage (Figure S7B). In this case, the polymer hydrophobicity was kept constant (50 PBO block units) and the highest values of membrane coverage and thickness were found when the copolymer was combined with lipids with a shorter hydrophobic tail.

The membrane coverage of the hybrid membranes obtained by SA was 5−8% lower than the one obtained with the LB method for similar membrane composition.[23] This is of crucial importance for the application of the SA method because it is a particularly appealing method for the generation of solid-supported membranes with a remarkable saving of time of preparation. Other structural and chemical parameters, such as glass transition temperature of the copolymers[64,65] and melting temperature and saturation of the lipids[28] might have influenced the polymer attachment onto the silica surface. However, the analysis of these parameters is beyond the scope of the present study.

2.3. Hybrid Membrane Morphology. To obtain information about the hybrid membrane morphology, we analyzed the hybrid membranes by AFM. Height and phase images of the hybrid membranes were acquired to (i) observe the phase domain separation, (ii) evaluate the thickness mismatch between the membrane domain, and (iii) measure

Table 2. Evaluation of the Morphological Properties of Different Polymer−Lipid Membranes Obtained by AFM Height and Phase Characterization and Comparison with the Membrane Coverage

lipid (50% w/w)	polymer (50% w/w)	phase separation	islands	domain mismatch (nm)	packing parameter (pure lipids)
DPPC	$PDMS_{61}$-$PMOXA_9$	yes	big[a]	7 ± 3	0.57[66,68]
	$PDMS_{89}$-$PMOXA_{10}$	yes	big	4−6 ± 1	
	PBO_{50}-PG_{18}	yes	small[b]	<1	
POPE	$PDMS_{61}$-$PMOXA_9$	no	big		0.66[68]
	$PDMS_{89}$-$PMOXA_{10}$	no	big		
	PBO_{50}-PG_{18}	no	big		
SM	$PDMS_{61}$-$PMOXA_9$	yes	small	6 ± 2	0.59[67]
	$PDMS_{89}$-$PMOXA_{10}$	no	small		
	PBO_{50}-PG_{18}	yes	small	4 ± 1	
NGPE	$PDMS_{61}$-$PMOXA_9$	no	no		0.41[68]
	$PDMS_{89}$-$PMOXA_{10}$	yes	small	6 ± 1	
	PBO_{50}-PG_{18}	no	small		

[a]"Big" island is within a size range of 30 ± 12 μm. [b]"Small" islands 8 ± 3 μm.
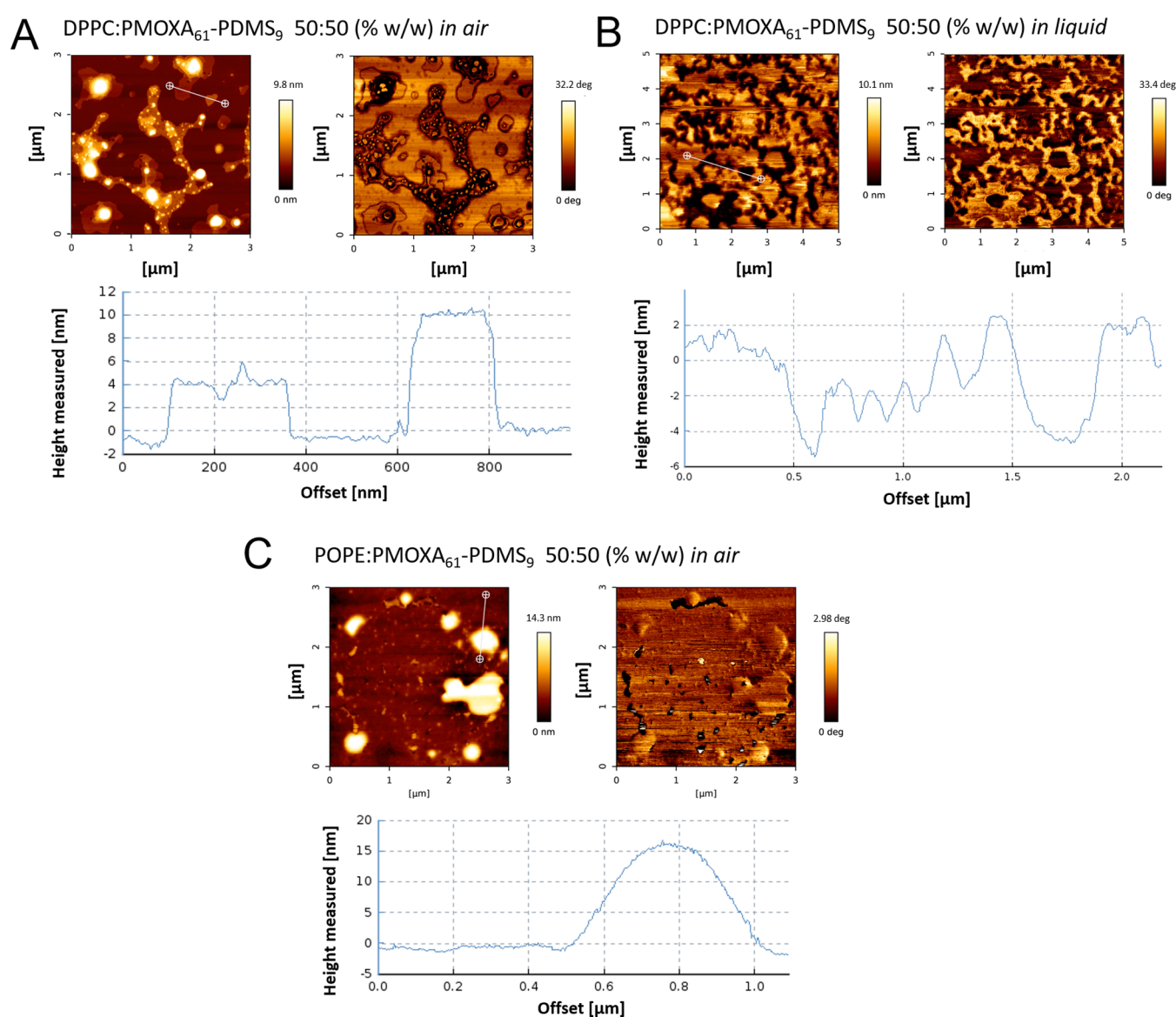

Figure 4. AFM height and comparison of phase images of membranes with good quality in terms of coverage and phase separation measured in air (A) and in liquid (B). Defected membranes were obtained with the SA method in the air (C). The presented AFM micrographs are representative of each case of hybrid membrane for which duplicates were conducted and 5 micrographs for each sample were recorded.

the height of copolymer domains surrounded by lipid environment, "islands", reported to be vesicle-like protrusions,[59] when the SA method is used.[18] Phase domain separation in the polymer−lipid hybrid membranes is the key aspect of preparing biomimetic materials, which mimics the presence of lipid rafts in cell membranes.

We present the main morphological characteristics of the phase domain separation and island formation for the different hybrid membranes obtained by AFM (Table 2). To better evaluate the morphological characteristics of the polymer−lipid planar assemblies, we also introduced PMOXA$_{89}$PMOXA$_{10}$.

We obtained a clear phase domain separation for all of the polymer−lipid hybrid assemblies except for the POPE lipid. AFM micrographs revealed that the combination of DPPC lipids with PDMS−PMOXA copolymers of either 61 or 89 PDMS units leads to a good quality hybrid membrane. In the case of the PDMS$_{89}$ hydrophobic block, the hybrid membrane presented a planar assembly with a clear phase domain separation. The AFM height profile showed a polymer−lipid mismatch for the phase domains of 4−6 ± 1 nm, with the polymer domain being higher than the lipid domain (Figure S8). Additionally, the domain separation obtained in dry conditions was very similar to the one of the same hybrid membrane obtained by a Langmuir−Blodgett preparation method.[22,23] The combination of DPPC with the copolymer having PDMS of 61 repeating units and the PBO$_{50}$−PG$_{18}$ copolymer, respectively, resulted in hybrid membranes with a defined phase membrane separation as well (Figures S8 and S9). Planar membrane architecture with the presence of polymer islands was determined for membranes from both copolymers. Due to the polymer conformation and the different hydrophobic/hydrophilic ratios of the blocks, the domain mismatch was different, 7 ± 3 nm for PDMS$_{61}$−PMOXA$_9$, while it was less than 1 nm for PBO−PG, which indicated a smoother membrane. SM was combined with PDMS$_{61}$−PMOXA$_9$, PDMS$_{89}$−PMOXA$_{10}$, and PBO$_{50}$−PG$_{18}$, respectively. The resulting hybrid membranes SM:PDMS$_{61}$−PMOXA$_9$ and SM:PBO$_{50}$−PG$_{18}$ were planar with phase domain separation (Figures S10−S12). The domain thickness mismatch was 6 ± 2 nm when the PDMS$_{61}$−PMOXA$_9$ copolymer was used, with defined lipid domains, irrespective of the PMOXA domains (Figure S10). On the other hand, SM:PDMS$_{89}$−PMOXA$_{10}$ did not show characteristics of phase separation and hybrid membrane formation.

These lipidic domains are embedded into a polymer matrix, as indicated by the darker color in the height profile. For DPPC and SM lipids, we reckon that they have the appropriate curvature to form a hybrid membrane with PDMS−PMOXA and PBO−PG copolymers.[69−71] Studies mainly focusing on lipid membrane characterization report that curvature is an essential parameter influencing the creation, stability, and size of "raftlike" lipid domains.[14,70,72−74] The combination of PDMS$_{89}$−PMOXA$_{10}$ and NGPE lipid resulted in a successful formation of hybrid membrane and phase domain separation. On the other hand, in the case of NGPE:PMOXA$_{61}$−PMOXA$_9$, we observed larger islands for a shorter hydrophobic polymer chain (Figure S13). Instead, when NGPE was combined with the PBO−PG copolymer, the AFM micrographs showed no membrane formation, rather the attachment of 3−4 nm diameter micelles onto the silica support (Figure S14). This can be attributed to the interaction between the PBO hydrophobic part of the polymer with NGPE, preventing

NGPE to form lipid domains at this specific copolymer-to-lipid ratio.[75]

An AFM comparison between a good quality membrane (high membrane coverage and clear phase separation) and a poor quality one (defective-containing membrane) indicates significant differences in the morphological characteristics and assembly of the two polymer−lipid mixtures. In DPPC:PMOXA$_{61}$−PDMS$_9$ hybrid membranes (Figure 4A), a clear phase domain separation was visible, with darker areas representing clusters of lipids entrapped within a polymer matrix, as reported for other hybrid membranes deposited with the LB method.[22,23]

The planar assembly was also clear for this combination, with a domain mismatch of 4−6 nm, in opposition to the 15−30 nm high vesicles assembly found for the hybrid POPE:PDMS$_{61}$−PMOXA$_9$ (Figure 4B).

On the contrary, when POPE was mixed with the PDMS−PMOXA (Figure 4B) or PBO−PG block copolymers (Figure S15), it does not create a hybrid membrane with clear domain separation between the polymeric and lipidic components. While we had indicative estimations regarding the membrane coverage and thickness based on QCM-D, they are not confirmed because we observed defects and big protrusions. It has been shown that, when objected to a planar bilayer conformation, lipids arrange in a "back-to-back" manner, which increases their curvature elastic stress.[70,76] This influences the morphology of the resulting membrane and therefore the ability of lipids to interact with other membrane components, which in our case are the copolymer parts. Among all of the tested lipids in our study, POPE is the one that fails to form a hybrid membrane and this can be associated with its large hydrophobic volume and negative curvature, leading to the formation of nonlamellar assemblies.[76,77] In comparison with the other lipids, POPE has a packing parameter of 0.66 (the packing parameters of the other lipids range from 0.4 to 0.59, Table 2). Moreover, at room temperature, POPE and particularly PE heads tend to densely pack.[78] This can explain the POPE behavior observed in our hybrid assemblies (Figure S15).[76,77] In particular, the ammonium group of the POPE head has just a weak electrostatic interaction with the phosphate group of another lipid and prefers to develop hydrogen bonds with the PMOXA or PG blocks of the amphiphilic block copolymers. This contributes to the POPE's failure to form lipid raftlike domains, as the lipid "diffuses" within the polymer membrane.[14] Phase and height images, acquired by AFM, show incomplete membrane formation and the presence of several islands or "fused vesicles" with height values between 15 and 30 nm. The absence of phase domain separation together with the instability in the air of the hybrid membranes formed when POPE is combined with the copolymers makes this lipid an inappropriate candidate for the preparation of biomimetic membrane platforms via the SA method. Concerning the other lipids used in this study, while NGPE can also form hydrogen bonds, we consider that the hydrophobic mismatch is more important in this particular case than the hydrogen bonding, and therefore, the determining factor in phase separation. On the other hand, the DPPC and SM lipids prefer to develop intrinsic lipid−lipid interactions. The strong electrostatic attraction between the quaternary ammonium groups of their polar heads and the phosphate moieties of the neighbor lipids is predominant in comparison with the hydrogen bonding leading to the formation of lipid−polymer domains in the hybrid membranes.

While the physical state and the structure of the lipids are important, the significant hydrophobic mismatch between lipid and polymer membranes has a very strong impact on the formation of planar hybrid membranes.

3. CONCLUSIONS

The solvent-assisted method is emerging as a promising method for fast and efficient solid-supported planar lipid and polymer membranes. Here, we expand the application of the SA method to hybrid membranes consisting of copolymers and lipids with the ultimate aim to understand and optimize the properties of the resulting hybrid membranes. We investigated the influence of various molecular characteristics such as lipid-to-copolymer ratio and the lengths of the copolymers and the lipid hydrophobic chains on the resulting quality and morphology of the hybrid membranes. Depending on the molecular factors, we obtain different average thicknesses of the membranes and observe the presence of lipid–polymer domain separation with different types of assemblies (e.g., islands). Using combinations of PDMS–PMOXA and PBO–PG diblock copolymers and lipids (DPPC, SM, POPE, and NGPE phospholipids), our findings suggest that the SA method is a compelling alternative for the development of solid-supported membranes and has the advantage of being straightforward and rapid. The use of the SA method for the generation of hybrid membranes further supports the creation of multifunctional hybrid membranes with distinct features of the lipid and polymer domains depending on their molecular factors and the desired application.

4. EXPERIMENTAL SECTION

4.1. Materials. Phospholipids POPE, SM, NGPE, and DPPC were purchased from Avanti Polar Lipids (Alabaster, AL). Phosphate-buffered saline (PBS), bovine serum albumin (BSA), and ethanol were purchased from Sigma-Aldrich (Switzerland). All of the diblock and triblock copolymers were synthesized by this research group.

4.2. Methods. *4.2.1. Synthesis of PDMS–PMOXA Diblock Copolymers.* The amphiphilic diblock copolymer PDMS–PMOXA was synthesized according to an established protocol:[17,79] mono-carbinol-functionalized PDMS-OH was synthesized by anionic ring-opening polymerization of hexamethylcyclotrisiloxane and end-group modification with 2-allyloxyethanol. The obtained PDMS-OH was activated with trifluoromethane sulfonic anhydride and chain-extended by cationic ring-opening polymerization with the MOXA monomer. Quenching with triethylamine/water to obtain hydroxy-functionalized PDMS–PMOXA–OH was performed, followed by end-group modification with succinic anhydride, leading to the final carboxy-functionalized PDMS–PMOXA–COOH.

All of the polymers used were characterized by ^{1}H NMR (Figures S1–S3).

4.2.2. Synthesis of PBO–PG. PBO–PG was synthesized according to an established protocol in two sequential microwave-based anionic ring-opening polymerizations:[50] PBO homopolymer was synthesized from butylene oxide monomer and potassium tert. butoxide. After quenching with methanol, the polymer was purified by extraction. Subsequently, the terminal hydroxy end group was deprotonated and the chain extension was performed with a protected glycidol derivative, 1-ethoxyethyl glycidyl ether (EEGE). After quenching with methanol, the protecting groups were removed in 0.1 M HCl. After purification by dialysis and lyophilization, the final PBO–PG diblock copolymer was obtained.

4.2.3. Nuclear Magnetic Resonance Spectroscopy (NMR). ^{1}H NMR spectra were recorded at 295 K in methanol-d4 (MeOD) or TMS-free chloroform-d1 (CDCl$_3$) (Cambridge Isotope Laboratories) on a 500 MHz Advance III NMR spectrometer (Bruker). The device was equipped with a BBFO SP FB standard probe and a default

number of 16 scans were used. The water signal in MeOD (4.87 ppm) or the residual solvent peak in CDCl$_3$ (7.26 ppm) were used for calibration. Processing of the spectra was performed in MestReNova software (version 11.0, Mestrelab, Spain).

4.2.4. Quartz Crystal Microbalance with Dissipation (QCM-D). QCM-D with Q-Sense E1 (Biolin Scientific, Sweden) setup was employed to monitor the membrane formation on the silica sensor. Changes in the resonance frequency (ΔF) and energy dissipation (ΔD) of the oscillating sensor chip as a function of time were simultaneously recorded at multiple odd overtones (3rd, 5th, 7th, 9th, and 11th). All data shown represent recordings at the seventh overtone. To estimate the hybrid membrane thickness and the mass of protein attached to the different membranes, the Sauerbrey equation was applied.[64] To apply the Sauerbrey equation, we observed that the recorded overtones were overlapping. This equation converts the frequency shift into mass using the relation $\Delta m = -C\Delta f$, where Δm is the mass, C is the proportionality constant (17.7 ng cm^{-2} Hz^{-1}), and Δf is the frequency shift. After establishing a baseline in the aqueous buffer solution, QCM-D measurements were conducted under continuous flow conditions. A flow rate of 50 μL/min was employed for the process of polymer, lipid, and BSA additions (steps 3 and 5, Figure 2). The same flow rate was also used for PBS and EtOH addition (steps 3 and 4, Figure 2). For baseline formation and rinsing steps, a flow rate of 100 μL/min was applied (steps 1 and 6). The flow was applied by a Reglo Digital peristaltic pump (Ismatec, Glattbrugg, Switzerland). The concentration of copolymers and lipids was 0.5 mg/L, as already optimized previously.[23,42] The QCM sensors used were QSX 303 SiO$_2$ and cleaned with Milli-Q water, 10% (w/w) SDS solution, or 10% (w/w) EtOH solution. Prior to the measurements, the sensors were treated with plasma (Nunc Lab-Tek Chamber Slide System, Thermo Fisher Scientific). The temperature of the flow cell was fixed at 24.0 $\pm$ 0.5 °C. BSA adsorption onto silicon dioxide led to a frequency shift of -24 ± 1 Hz (Figure S16) and represents the control measurement to compare with the BSA adsorption onto polymer membranes. Q-Sense Dfind software was used for data analysis.

4.2.5. Atomic Force Microscopy (AFM). AFM was performed with JPK NanoWizard 3 AFM (JPK Instruments AG, Germany). The AC mode topography images were obtained in the air using silicon cantilevers (Tap150 Al-G, Budget Sensors) with a nominal spring constant of 10–130 Nm^{-1} and a resonance frequency of 150 kHz. The images were analyzed with the data analysis software JPK Data Processing (v. 5.0).

4.2.6. Hybrid Membrane Formation for AFM Analysis. All of the hybrid membranes for AFM measurements were obtained with a homemade device. The device consists of a chamber with two compartments (1 cm^2 each) for hosting the cut silica wafer and allowed the simultaneous preparation of two membranes per experiment, under the established SA protocol. The chamber was connected to a digital peristaltic pump (Ismatec, Glattbrugg, Switzerland) and sealed. The solutions were injected at a constant flow following the same procedures adopted for the QCM-D measurements. Frequency shift values for membrane formation and BSA step of different hybrid membranes composed of polymer and lipids are reported and membrane thickness and coverage were calculated (Table S1, Figures S1–S16)

ASSOCIATED CONTENT

Ⓢ Supporting Information

The Supporting Information is available free of charge at https://pubs.acs.org/doi/10.1021/acs.langmuir.2c00204.

> Polymer NMR and structure; formation and characterization of solid-supported lipid-polymer membrane by QCM-D; morphlogy of the hybrid membranes by AFM; BSA attachment; Frequency Shift, Dissipation and Membrane Thickness values for the hybrid membranes (PDF)

■ AUTHOR INFORMATION

Corresponding Authors

    Wolfgang P. Meier − *Department of Chemistry, University of Basel, 4058 Basel, Switzerland; National Centre of Competence in Research Molecular Systems Engineering (NCCR MSE), 4058 Basel, Switzerland;* ⦿ orcid.org/0000-0002-7551-8272; Email: wolfgang.meier@unibas.ch

    Cornelia G. Palivan − *Department of Chemistry, University of Basel, 4058 Basel, Switzerland; National Centre of Competence in Research Molecular Systems Engineering (NCCR MSE), 4058 Basel, Switzerland;* ⦿ orcid.org/0000-0001-7777-5355; Email: cornelia.palivan@unibas.ch

Authors

    Stefano Di Leone − *Department of Chemistry, University of Basel, 4058 Basel, Switzerland; School of Life Sciences, Institute for Chemistry and Bioanalytics, University of Applied Sciences Northwestern Switzerland (FHNW), 4132 Muttenz, Switzerland*

    Myrto Kyropoulou − *Department of Chemistry, University of Basel, 4058 Basel, Switzerland; National Centre of Competence in Research Molecular Systems Engineering (NCCR MSE), 4058 Basel, Switzerland*

    Julian Köchlin − *Department of Chemistry, University of Basel, 4058 Basel, Switzerland*

    Riccardo Wehr − *Department of Chemistry, University of Basel, 4058 Basel, Switzerland*

Complete contact information is available at:
https://pubs.acs.org/10.1021/acs.langmuir.2c00204

Author Contributions

∥S.D.L. and M.K. contributed equally to this work.

Notes

The authors declare no competing financial interest.

■ REFERENCES

(1) Zhang, X.; Tanner, P.; Graff, A.; Palivan, C. G.; Meier, W. Mimicking the Cell Membrane with Block Copolymer Membranes. *J. Polym. Sci., Part A: Polym. Chem.* **2012**, *50*, 2293−2318.

(2) Kowal, J.; Zhang, X.; Dinu, I. A.; Palivan, C. G.; Meier, W. Planar Biomimetic Membranes Based on Amphiphilic Block Copolymers. *ACS Macro Lett.* **2014**, *3*, 59−63.

(3) Taubert, A.; Napoli, A.; Meier, W. Self-Assembly of Reactive Amphiphilic Block Copolymers as Mimetics for Biological Membranes. *Curr. Opin. Chem. Biol.* **2004**, *8*, 598−603.

(4) Fauquignon, M.; Ibarboure, E.; Le Meins, J.-F. Membrane Reinforcement in Giant Hybrid Polymer Lipid Vesicles Achieved by Controlling the Polymer Architecture. *Soft Matter* **2021**, *17*, 83−89.

(5) Chimisso, V.; Maffeis, V.; Hürlimann, D.; Palivan, C. G.; Meier, W. Self-Assembled Polymeric Membranes and Nanoassemblies on Surfaces: Preparation, Characterization, and Current Applications. *Macromol. Biosci.* **2020**, *20*, No. 1900257.

(6) Shen, Y.-x.; Saboe, P. O.; Sines, I. T.; Erbakan, M.; Kumar, M. Biomimetic Membranes: A Review. *J. Membr. Sci.* **2014**, *454*, 359−381.

(7) Nielsen, C. H. Biomimetic Membranes for Sensor and Separation Applications. *Anal. Bioanal. Chem.* **2009**, *395*, 697−718.

(8) Piletsky, S. A.; Panasyuk, T. L.; Piletskaya, E. V.; Nicholls, I. A.; Ulbricht, M. Receptor and Transport Properties of Imprinted Polymer Membranes—a Review. *J. Membr. Sci.* **1999**, *157*, 263−278.

(9) Schulz, M.; Werner, S.; Bacia, K.; Binder, W. H. Controlling Molecular Recognition with Lipid/Polymer Domains in Vesicle Membranes. *Angew. Chem., Int. Ed.* **2013**, *52*, 1829−1833.

(10) Davies, M. L.; Hamilton, C. J.; Murphy, S. M.; Tighe, B. J. Polymer Membranes in Clinical Sensor Applications. *Biomaterials* **1992**, *13*, 971−978.

(11) Clodt, J. I.; Filiz, V.; Rangou, S.; Buhr, K.; Abetz, C.; Höche, D.; Hahn, J.; Jung, A.; Abetz, V. Double Stimuli-Responsive Isoporous Membranes via Post-Modification of PH-Sensitive Self-Assembled Diblock Copolymer Membranes. *Adv. Funct. Mater.* **2013**, *23*, 731−738.

(12) Ozaydin-Ince, G.; Coclite, A. M.; Gleason, K. K. CVD of Polymeric Thin Films: Applications in Sensors, Biotechnology, Microelectronics/Organic Electronics, Microfluidics, MEMS, Composites and Membranes. *Rep. Prog. Phys.* **2012**, *75*, No. 016501.

(13) Zhang, X.; Higashihara, T.; Ueda, M.; Wang, L. Polyphenylenes and the Related Copolymer Membranes for Electrochemical Device Applications. *Polym. Chem.* **2014**, *5*, 6121−6141.

(14) Le Meins, J.-F.; Schatz, C.; Lecommandoux, S.; Sandre, O. Hybrid Polymer/Lipid Vesicles: State of the Art and Future Perspectives. *Mater. Today* **2013**, *16*, 397−402.

(15) Chemin, M.; Brun, P.-M.; Lecommandoux, S.; Sandre, O.; Le Meins, J.-F. Hybrid Polymer/Lipid Vesicles: Fine Control of the Lipid and Polymer Distribution in the Binary Membrane. *Soft Matter* **2012**, *8*, 2867−2874.

(16) Rao, S.; Prestidge, C. A. Polymer-Lipid Hybrid Systems: Merging the Benefits of Polymeric and Lipid-Based Nanocarriers to Improve Oral Drug Delivery. *Expert Opin. Drug Delivery* **2016**, *13*, 691−707.

(17) Wu, D.; Spulber, M.; Itel, F.; Chami, M.; Pfohl, T.; Palivan, C. G.; Meier, W. Effect of Molecular Parameters on the Architecture and Membrane Properties of 3D Assemblies of Amphiphilic Copolymers. *Macromolecules* **2014**, *47*, 5060−5069.

(18) Jaskiewicz, K.; Makowski, M.; Kappl, M.; Landfester, K.; Kroeger, A. Mechanical Properties of Poly(Dimethylsiloxane)-*Block*-Poly(2-Methyloxazoline) Polymersomes Probed by Atomic Force Microscopy. *Langmuir* **2012**, *28*, 12629−12636.

(19) Blanazs, A.; Armes, S. P.; Ryan, A. J. Self-Assembled Block Copolymer Aggregates: From Micelles to Vesicles and Their Biological Applications. *Macromol. Rapid Commun.* **2009**, *30*, 267−277.

(20) Bangham, A. D. Membrane Models with Phospholipids. *Prog. Biophys. Mol. Biol.* **1968**, *18*, 29−95.

(21) Schulz, M.; Olubummo, A.; Bacia, K.; Binder, W. H. Lateral Surface Engineering of Hybrid Lipid−BCP Vesicles and Selective Nanoparticle Embedding. *Soft Matter* **2014**, *10*, 831−839.

(22) Kowal, J.; Wu, D.; Mikhalevich, V.; Palivan, C. G.; Meier, W. Hybrid Polymer−Lipid Films as Platforms for Directed Membrane Protein Insertion. *Langmuir* **2015**, *31*, 4868−4877.

(23) Di Leone, S.; Avsar, S. Y.; Belluati, A.; Wehr, R.; Palivan, C. G.; Meier, W. Polymer−Lipid Hybrid Membranes as a Model Platform to Drive Membrane−Cytochrome *c* Interaction and Peroxidase-like Activity. *J. Phys. Chem. B* **2020**, *124*, 4454−4465.

(24) Jagoda, A.; Ketikidis, P.; Zinn, M.; Meier, W.; Kita-Tokarczyk, K. Interactions of Biodegradable Poly([R]-3-Hydroxy-10-Undecenoate) with 1,2-Dioleoyl-*Sn*-Glycero-3-Phosphocholine Lipid: A Monolayer Study. *Langmuir* **2011**, *27*, 10878−10885.

(25) Tanaka, M.; Sackmann, E. Polymer-Supported Membranes as Models of the Cell Surface. *Nature* **2005**, *437*, 656−663.

(26) Castellana, E. T.; Cremer, P. S. Solid Supported Lipid Bilayers: From Biophysical Studies to Sensor Design. *Surf. Sci. Rep.* **2006**, *61*, 429−444.

(27) Richter, R. P.; Bérat, R.; Brisson, A. R. Formation of Solid-Supported Lipid Bilayers: An Integrated View. *Langmuir* **2006**, *22*, 3497−3505.

(28) Bakht, O.; Pathak, P.; London, E. Effect of the Structure of Lipids Favoring Disordered Domain Formation on the Stability of Cholesterol-Containing Ordered Domains (Lipid Rafts): Identification of Multiple Raft-Stabilization Mechanisms. *Biophys. J.* **2007**, *93*, 4307−4318.

(29) Åkesson, A.; Lind, T.; Ehrlich, N.; Stamou, D.; Wacklin, H.; Cárdenas, M. Composition and Structure of Mixed Phospholipid Supported Bilayers Formed by POPC and DPPC. *Soft Matter* **2012**, *8*, 5658−5665.

(30) Mumtaz Virk, M.; Hofmann, B.; Reimhult, E. Formation and Characteristics of Lipid-Blended Block Copolymer Bilayers on a Solid Support Investigated by Quartz Crystal Microbalance and Atomic Force Microscopy. *Langmuir* **2019**, *35*, 739−749.

(31) Dao, T. P. T.; Fernandes, F.; Er-Rafik, M.; Salva, R.; Schmutz, M.; Brûlet, A.; Prieto, M.; Sandre, O.; Le Meins, J.-F. Phase Separation and Nanodomain Formation in Hybrid Polymer/Lipid Vesicles. *ACS Macro Lett.* **2015**, *4*, 182−186.

(32) Schwartz, D. K. Langmuir-Blodgett Film Structure. *Surf. Sci. Rep.* **1997**, *27*, 245−334.

(33) Kyropoulou, M.; Yorulmaz Avsar, S.; Schoenenberger, C.-A.; Palivan, C. G.; Meier, W. P. From Spherical Compartments to Polymer Films: Exploiting Vesicle Fusion to Generate Solid Supported Thin Polymer Membranes. *Nanoscale* **2021**, *13*, 6944−6952.

(34) Jackman, J. A.; Cho, N.-J. Supported Lipid Bilayer Formation: Beyond Vesicle Fusion. *Langmuir* **2020**, *36*, 1387−1400.

(35) Dörr, J. M.; Scheidelaar, S.; Koorengevel, M. C.; Dominguez, J. J.; Schäfer, M.; van Walree, C. A.; Killian, J. A. The Styrene−Maleic Acid Copolymer: A Versatile Tool in Membrane Research. *Eur. Biophys. J.* **2016**, *45*, 3−21.

(36) He, L.; Robertson, J. W. F.; Li, J.; Kärcher, I.; Schiller, S. M.; Knoll, W.; Naumann, R. Tethered Bilayer Lipid Membranes Based on Monolayers of Thiolipids Mixed with a Complementary Dilution Molecule. 1. Incorporation of Channel Peptides. *Langmuir* **2005**, *21*, 11666−11672.

(37) Preta, G.; Jankunec, M.; Heinrich, F.; Griffin, S.; Sheldon, I. M.; Valincius, G. Tethered Bilayer Membranes as a Complementary Tool for Functional and Structural Studies: The Pyolysin Case. *Biochim. Biophys. Acta, Biomembr.* **2016**, *1858*, 2070−2080.

(38) Tabaei, S. R.; Choi, J.-H.; Haw Zan, G.; Zhdanov, V. P.; Cho, N.-J. Solvent-Assisted Lipid Bilayer Formation on Silicon Dioxide and Gold. *Langmuir* **2014**, *30*, 10363−10373.

(39) Tabaei, S. R.; Jackman, J. A.; Kim, S.-O.; Zhdanov, V. P.; Cho, N.-J. Solvent-Assisted Lipid Self-Assembly at Hydrophilic Surfaces: Factors Influencing the Formation of Supported Membranes. *Langmuir* **2015**, *31*, 3125−3134.

(40) Tabaei, S. R.; Jackman, J. A.; Kim, M.; Yorulmaz, S.; Vafaei, S.; Cho, N.-J. Biomembrane Fabrication by the Solvent-Assisted Lipid Bilayer (SALB) Method. *J. Visualized Exp.* **2015**, No. 53073.

(41) Ferhan, A. R.; Yoon, B. K.; Park, S.; Sut, T. N.; Chin, H.; Park, J. H.; Jackman, J. A.; Cho, N.-J. Solvent-Assisted Preparation of Supported Lipid Bilayers. *Nat. Protoc.* **2019**, *14*, 2091−2118.

(42) Di Leone, S.; Vallapurackal, J.; Yorulmaz Avsar, S.; Kyropolou, M.; Ward, T. R.; Palivan, C. G.; Meier, W. Expanding the Potential of the Solvent-Assisted Method to Create Bio-Interfaces from Amphiphilic Block Copolymers. *Biomacromolecules* **2021**, *22*, 3005−3016.

(43) Khakbaz, P.; Klauda, J. B. Probing the Importance of Lipid Diversity in Cell Membranes via Molecular Simulation. *Chem. Phys. Lipids* **2015**, *192*, 12−22.

(44) Ehrsam, D.; Porta, F.; Hussner, J.; Seibert, I.; Meyer zu Schwabedissen, H. E. PDMS-PMOXA-Nanoparticles Featuring a Cathepsin B-Triggered Release Mechanism. *Materials* **2019**, *12*, No. 2836.

(45) Gunkel-Grabole, G.; Sigg, S.; Lomora, M.; Lörcher, S.; Palivan, C. G.; Meier, W. P. Polymeric 3D Nano-Architectures for Transport and Delivery of Therapeutically Relevant Biomacromolecules. *Biomater. Sci.* **2015**, *3*, 25−40.

(46) Gunkel-Grabole, G.; Palivan, C.; Meier, W. Nanostructured Surfaces through Immobilization of Self-Assembled Polymer Architectures Using Thiol−Ene Chemistry. *Macromol. Mater. Eng.* **2017**, *302*, No. 1600363.

(47) Garni, M.; Wehr, R.; Avsar, S. Y.; John, C.; Palivan, C.; Meier, W. Polymer Membranes as Templates for Bio-Applications Ranging from Artificial Cells to Active Surfaces. *Eur. Polym. J.* **2019**, *112*, 346−364.

(48) Tribet, C.; Vial, F. Flexible Macromolecules Attached to Lipid Bilayers: Impact on Fluidity, Curvature, Permeability and Stability of the Membranes. *Soft Matter* **2008**, *4*, 68−81.

(49) Le Meins, J.-F.; Schatz, C.; Lecommandoux, S.; Sandre, O. Hybrid Polymer/Lipid Vesicles: State of the Art and Future Perspectives. *Mater. Today* **2013**, *16*, 397−402.

(50) Wehr, R.; Gaitzsch, J.; Daubian, D.; Fodor, C.; Meier, W. Deepening the Insight into Poly(Butylene Oxide)-*Block*-Poly-(Glycidol) Synthesis and Self-Assemblies: Micelles, Worms and Vesicles. *RSC Adv.* **2020**, *10*, 22701−22711.

(51) Bakardzhiev, P.; Momekova, D.; Edwards, K.; Konstantinov, S.; Rangelov, S. Novel Polyglycidol-Lipid Conjugates Create a Stabilizing Hydrogen-Bonded Layer around Cholesterol-Containing Dipalmitoyl Phosphatidylcholine Liposomes. *J. Drug Delivery Sci. Technol.* **2015**, *29*, 90−98.

(52) Konradi, R.; Pidhatika, B.; Mühlebach, A.; Textor, M. Poly-2-Methyl-2-Oxazoline: A Peptide-like Polymer for Protein-Repellent Surfaces. *Langmuir* **2008**, *24*, 613−616.

(53) Nardin, C.; Hirt, T.; Leukel, J.; Meier, W. Polymerized ABA Triblock Copolymer Vesicles. *Langmuir* **2000**, *16*, 1035−1041.

(54) Dao, T. P. T.; Brûlet, A.; Fernandes, F.; Er-Rafik, M.; Ferji, K.; Schweins, R.; Chapel, J.-P.; Fedorov, A.; Schmutz, M.; Prieto, M.; Sandre, O.; Le Meins, J.-F. Mixing Block Copolymers with Phospholipids at the Nanoscale: From Hybrid Polymer/Lipid Wormlike Micelles to Vesicles Presenting Lipid Nanodomains. *Langmuir* **2017**, *33*, 1705−1715.

(55) Khan, A. K.; Ho, J. C. S.; Roy, S.; Liedberg, B.; Nallani, M. Facile Mixing of Phospholipids Promotes Self-Assembly of Low-Molecular-Weight Biodegradable Block Co-Polymers into Functional Vesicular Architectures. *Polymers* **2020**, *12*, No. 979.

(56) Go, Y. K.; Kambar, N.; Leal, C. Hybrid Unilamellar Vesicles of Phospholipids and Block Copolymers with Crystalline Domains. *Polymers* **2020**, *12*, No. 1232.

(57) Li, Y.; Chen, X.; Gu, N. Computational Investigation of Interaction between Nanoparticles and Membranes: Hydrophobic/Hydrophilic Effect. *J. Phys. Chem. B* **2008**, *112*, 16647−16653.

(58) Dao, T. P. T.; Fernandes, F.; Ibarboure, E.; Ferji, K.; Prieto, M.; Sandre, O.; Le Meins, J.-F. Modulation of Phase Separation at the Micron Scale and Nanoscale in Giant Polymer/Lipid Hybrid Unilamellar Vesicles (GHUVs). *Soft Matter* **2017**, *13*, 627−637.

(59) Le Meins, J.-F.; Sandre, O.; Lecommandoux, S. Recent Trends in the Tuning of Polymersomes' Membrane Properties. *Eur. Phys. J. E* **2011**, *34*, No. 14.

(60) Grason, G. The Packing of Soft Materials: Molecular Asymmetry, Geometric Frustration and Optimal Lattices in Block Copolymer Melts. *Phys. Rep.* **2006**, *433*, 1−64.

(61) Tsai, H.-C.; Yang, Y.-L.; Sheng, Y.-J.; Tsao, H.-K. Formation of Asymmetric and Symmetric Hybrid Membranes of Lipids and Triblock Copolymers. *Polymers* **2020**, *12*, No. 639.

(62) Dionzou, M.; Morère, A.; Roux, C.; Lonetti, B.; Marty, J.-D.; Mingotaud, C.; Joseph, P.; Goudounèche, D.; Payré, B.; Léonetti, M.; Mingotaud, A. F. Comparison of Methods for the Fabrication and the Characterization of Polymer Self-Assemblies: What Are the Important Parameters? *Soft Matter* **2016**, *12*, 2166−2176.

(63) Itel, F.; Najer, A.; Palivan, C. G.; Meier, W. Dynamics of Membrane Proteins within Synthetic Polymer Membranes with Large Hydrophobic Mismatch. *Nano Lett.* **2015**, *15*, 3871−3878.

(64) Jiménez, Y.; Otero, M.; Arnau, A. QCM Data Analysis and Interpretation. In *Piezoelectric Transducers and Applications*, Vives, A. A., Ed.; Springer: Berlin, Heidelberg, 2008; pp 331−398.

(65) Shahane, G.; Ding, W.; Palaiokostas, M.; Orsi, M. Physical Properties of Model Biological Lipid Bilayers: Insights from All-Atom Molecular Dynamics Simulations. *J Mol. Model.* **2019**, *25*, No. 76.

(66) Jurak, M.; Mroczka, R.; Łopucki, R. Properties of Artificial Phospholipid Membranes Containing Lauryl Gallate or Cholesterol. *J. Membr. Biol.* **2018**, *251*, 277−294.

(67) Kobierski, J.; Wnętrzak, A.; Chachaj-Brekiesz, A.; Dynarowicz-Latka, P. Predicting the Packing Parameter for Lipids in Monolayers with the Use of Molecular Dynamics. *Colloids Surf., B* **2022**, *211*, No. 112298.

(68) Yoshimoto, M.; Sakamoto, H.; Shirakami, H. Covalent Conjugation of Tetrameric Bovine Liver Catalase to Liposome Membranes for Stabilization of the Enzyme Tertiary and Quaternary Structures. *Colloids Surf., B* **2009**, *69*, 281−287.

(69) van Meer, G.; Voelker, D. R.; Feigenson, G. W. Membrane Lipids: Where They Are and How They Behave. *Nat. Rev. Mol. Cell Biol.* **2008**, *9*, 112−124.

(70) Callan-Jones, A.; Bassereau, P. Curvature-Driven Membrane Lipid and Protein Distribution. *Curr. Opin. Solid State Mater. Sci.* **2013**, *17*, 143−150.

(71) Cooke, I. R.; Deserno, M. Coupling between Lipid Shape and Membrane Curvature. *Biophys. J.* **2006**, *91*, 487−495.

(72) Semrau, S.; Idema, T.; Schmidt, T.; Storm, C. Membrane-Mediated Interactions Measured Using Membrane Domains. *Biophys. J.* **2009**, *96*, 4906−4915.

(73) Zhang, W.; Coughlin, M. L.; Metzger, J. M.; Hackel, B. J.; Bates, F. S.; Lodge, T. P. Influence of Cholesterol and Bilayer Curvature on the Interaction of PPO−PEO Block Copolymers with Liposomes. *Langmuir* **2019**, *35*, 7231−7241.

(74) Risselada, H. J.; Marrink, S. J. Curvature Effects on Lipid Packing and Dynamics in Liposomes Revealed by Coarse Grained Molecular Dynamics Simulations. *Phys. Chem. Chem. Phys.* **2009**, *11*, 2056−2067.

(75) Hammons, J. A.; Ingólfsson, H. I.; Lee, J. R. I.; Carpenter, T. S.; Sanborn, J.; Tunuguntla, R.; Yao, Y.-C.; Weiss, T. M.; Noy, A.; Van Buuren, T. Decoupling Copolymer, Lipid and Carbon Nanotube Interactions in Hybrid, Biomimetic Vesicles. *Nanoscale* **2020**, *12*, 6545−6555.

(76) Koller, D.; Lohner, K. The Role of Spontaneous Lipid Curvature in the Interaction of Interfacially Active Peptides with Membranes. *Biochim. Biophys. Acta, Biomembr.* **2014**, *1838*, 2250−2259.

(77) Kollmitzer, B.; Heftberger, P.; Rappolt, M.; Pabst, G. Monolayer Spontaneous Curvature of Raft-Forming Membrane Lipids. *Soft Matter* **2013**, *9*, 10877−10884.

(78) Leekumjorn, S.; Sum, A. K. Molecular Characterization of Gel and Liquid-Crystalline Structures of Fully Hydrated POPC and POPE Bilayers. *J. Phys. Chem. B* **2007**, *111*, 6026−6033.

(79) Egli, S.; Nussbaumer, M. G.; Balasubramanian, V.; Chami, M.; Bruns, N.; Palivan, C.; Meier, W. Biocompatible Functionalization of Polymersome Surfaces: A New Approach to Surface Immobilization and Cell Targeting Using Polymersomes. *J. Am. Chem. Soc.* **2011**, *133*, 4476−4483.